

Article

Synthesis and Photovoltaic Properties of 2D-Conjugated Polymers Based on Alkylthiothienyl-Substituted Benzodithiophene and Different Accepting Units

Xunchang Wang ¹, Chang Cheng ¹, Yuda Li ¹ and Feng Wang ^{1,2,*}

¹ Key Laboratory for Green Chemical Process of Ministry of Education, Wuhan Institute of Technology, Wuhan 430073, China; wang_xc@qibebt.ac.cn (X.W.); cc21029648@gmail.com (C.C.); psydli@163.com (Y.L.)

² Hubei Novel Reactor & Green Chemical Technology Key Laboratory, Wuhan Institute of Technology, Wuhan 430073, China

* Correspondence: pswang@wit.edu.cn; Tel.: +86-27-8719-4980

Received: 24 February 2018; Accepted: 15 March 2018; Published: 18 March 2018

Abstract: Two new low bandgap conjugated polymers, PBDTS-ID and PBDTS-DTNT, containing isoindigo (ID) and naphtho[1,2-*c*:5,6-*c'*]bis[1,2,5]thiadiazole (NT), respectively, as an electron-deficient unit and alkylthiothienyl-substituted benzodithiophene (BDTS) as an electron-rich unit, were designed and synthesized by palladium-catalyzed Stille polycondensation. Both polymers showed good thermal stability up to 330 °C and broad absorption ranging from 300 to 842 nm. Electrochemical measurement revealed that PBDTS-ID and PBDTS-DTNT exhibited relatively low-lying highest occupied molecular orbital energy levels at -5.40 and -5.24 eV, respectively. These features might be beneficial for obtaining reasonable high open-circuit voltage and high short-circuit current. Polymer solar cells (PSCs) were fabricated with an inverted structure of indium-tin oxide/poly(ethylenimine ethoxylate)/polymer:PC₇₁BM/MoO₃/Ag. As a preliminary result, the PSCs based on PBDTS-ID and PBDTS-DTNT exhibited moderate power conversion efficiencies of 2.70% and 2.71%, respectively.

Keywords: conjugated polymers; polymer solar cells; inverted structure; power conversion efficiency

1. Introduction

Nowadays, polymer solar cells (PSCs) as a promising clean and renewable energy have attracted considerable attention owing to their manufacturing advantages such as light weight, low cost, flexibility, and ease of processing [1–7]. To enhance the photovoltaic performance of PSCs, numerous effective strategies have been performed to develop novel conjugated polymers containing electron-rich donor (D) and electron-poor acceptor (A) units with optimized highest occupied molecular orbital (HOMO)/lowest unoccupied molecular orbital (LUMO) energy levels. More encouragingly, PSCs with excellent power conversion efficiencies (PCEs) up to 13% have been reported [8].

Benzodithiophene (BDT) is one of the most widely used structural units for donor polymers in PSCs because of its rigid and large planar structure [8–28]. Recently, side chains of BDT-containing conjugated polymers have been found to play a critical role in affecting polymer packing and bulk heterojunction (BHJ) morphology. In comparison with alkoxy functionalized BDT, the conjugated polymer with alkylthienyl functionalized BDT can effectively tune the solubility, absorption bands, electronic energy levels, and carrier mobilities [29]. Alternatively, the sulfur atom possesses π -acceptor ability because of the unique $p_{\pi}(\text{C})-d_{\pi}(\text{S})$ orbital overlap between the alkylthio substitution and the $-\text{C}=\text{C}-$ double bond [30]. Therefore, the introduction of an alkylthiothienyl side chain to the BDT unit is for an important issue in BDT-containing conjugated polymers that could determine their photovoltaic performance. The two-dimensional (2D) BDT-thieno[3,4-*b*]thiophene (TT) copolymer

reported by Li et al. achieved a PCE of 8.42% with a high open-circuit voltage (V_{OC}) of 0.84 V. The enhanced V_{OC} value of 0.84 V for the PSC, achieved by introducing an alkylthiothienyl side chain, should arise from the down-shifted HOMO energy level of the polymer [30]. Subsequently, Hou and coworkers synthesized a novel alkylthiothienyl-substituted polymer PBDTTS1, and a higher PCE of 9.48% was achieved by replacing the branched alkyls (2-ethylhexyl) with linear alkyls (octyl), resulting in a superior absorption spectrum and enhanced hole mobility [17]. Recently, Sun et al. designed and synthesized a wide bandgap copolymer, PBT1-EH, which was optimized by an alkylthiothienyl side chain and thus a PCE of 10.6% was obtained [31]. These reports inspired us to rationally design a new alkylthiothienyl-substituted BDT-based conjugated polymer for high performance PSCs with high V_{OC} and short-circuit current (J_{SC}).

As for the electron-poor acceptor units in the D–A photovoltaic polymers, isoindigo (ID) has attracted much attention because of its strong electron-withdrawing ability and the inherent advantages of its two indolone structures [21,32–42]. Naphtho[1,2-*c*:5,6-*c'*]bis[1,2,5]thiadiazole (NT), a benzothiadiazole-fused heteroaromatic unit, exhibited potential application in designing D–A conjugated polymers due to its thermal stability, broad optical absorption, and high electron-withdrawing effect [38,39,43–53].

Herein, we designed and prepared two novel D–A polymers, PBDTS-ID and PBDTS-DTNT, with alkylthiothienyl-BDT (BDTS) as a donor unit and ID or NT as an acceptor unit (see Scheme 1). The thermogravimetric analysis (TGA), UV-Vis absorption spectroscopy, electrochemical cyclic voltammetry (CV), and morphological properties of the polymers PBDTS-ID and PBDTS-DTNT were systematically characterized. The two polymers exhibited a deeper HOMO energy level of -5.40 eV for PBDTS-ID and -5.24 eV for PBDTS-DTNT, and broad absorption in the wavelength range from 300 to 842 nm. As a result, PSCs fabricated with PBDTS-ID as a donor and PC₇₁BM as an acceptor exhibited a high V_{OC} of 0.84 V, leading to a moderate PCE of 2.70% under the excitation of standard AM 1.5 G spectrum at $100 \text{ mW}\cdot\text{cm}^{-2}$. Meanwhile, the V_{OC} , J_{SC} , and PCE of the PSCs based on the optimized fabrication conditions were 0.72 V, $8.31 \text{ mA}\cdot\text{cm}^{-2}$, and 2.71%, respectively, for the PBDTS-DTNT polymer.

2. Materials and Methods

2.1. Materials

All reagents were obtained from Aladdin Reagent Co. Ltd. (Shanghai, China), and Sigma-Aldrich Co. (Shanghai, China), and were used without further purification. Tetrahydrofuran (THF) and toluene were freshly distilled from sodium under a nitrogen atmosphere for use. Monomers M1, M2, and M3 were prepared and characterized according to the published procedures [17,34,50].

2.2. Characterization

Nuclear magnetic resonance (NMR) spectra were collected on a Bruker Advance III 600 (Bruker Co., Rheinstetten, Germany) with tetramethylsilane as a reference. Elemental analysis was carried out on a Vario EL III CHN elemental analyzer (Elementar Co., Langenselbold, Germany). Weight-average (M_w) and number-average (M_n) molecular weights of the polymers were determined on an Agilent in THF using a calibration curve of the polystyrene standards (Milford, MA, USA). The thermal properties of the polymers were evaluated on a TA instrument Q600-0825 (Waters Ltd, Hertfordshire, United Kingdom) under a nitrogen atmosphere with a heating rate of $10 \text{ }^\circ\text{C}\cdot\text{min}^{-1}$. Powder X-ray diffraction patterns were obtained on a Bruker D8 Advance (Bruker Co., Karlsruhe, Germany). Absorption spectra were recorded on a UV-3100PC spectrophotometer (Shimadzu Co., Kyoto, Japan). CV was carried out on a CHI electrochemical workstation (Chenhua, Shanghai, China), and sn Ag/AgCl electrode, platinum wire, and glassy carbon were used as the reference electrode, counter electrode, and working electrode, respectively. The atomic force microscopy (AFM) patterns were obtained on a NanoScope NS3A system in tapping-mode (Veeco Inc., Santa Barbara, CA, USA).

The transmission electron microscopy (TEM) patterns were obtained on a HITACHI H-7650 electron microscope using a 100-kV acceleration voltage (Hitachi Co., Tokyo, Japan).

2.3. Device Fabrication

The PSCs were fabricated with the structure indium-tin oxide (ITO)/poly(ethylenimine ethoxylate) (PEIE)/polymer:PC₇₁BM/MoO₃/Ag. The ITO glasses were cleaned with a surfactant scrub, and washed sequentially by deionized water, acetone, and isopropanol. Oxygen plasma treatment was conducted on the ITO substrates for 5 min. A PEIE thin layer was spin-coated on pretreated ITO-coated glass substrates and annealed at 100 °C in air for 5 min, after which the polymer:PC₇₁BM (different weight ratio) solution was spin-coated onto the PEIE layer at a concentration of 6 mg·mL⁻¹. After drying the solvent, MoO₃ (10 nm) and Ag (100 nm) were successively evaporated through a shadow mask on top of the active layer, under a vacuum of 10⁻⁵ Pa. The current density–voltage (*J*–*V*) characteristics were recorded with a sourcemeter 2400 (Keithley Co, New York, NY, USA) controlled by a LabVIEW program in a nitrogen-filled glove box under white light illumination (100 mW·cm⁻²). The spectral responses of PSCs were recorded using a commercial external quantum efficiency (EQE)/incident photon-to-charge carrier efficiency (IPCE) setup (7-SCSpecIII, Beijing 7-star, Beijing, China).

2.4. Polymer Synthesis

2.4.1. Synthesis of PBDTS-ID

M1 (193.7 mg, 0.2 mmol) and M2 (168.2 mg, 0.2 mmol) were dissolved in a mixed solvent of freshly distilled toluene (10 mL) and anhydrous *N,N*-dimethylformamide (DMF) (2 mL). The mixture was purged with argon for 10 min, and then Pd(dba)₂ (3 mg) and tris(3-methoxyphenyl)phosphine (6 mg) were added into the flask as a catalyst. After being purged for another 10 min, the reaction mixture was heated to 110 °C for 24 h under an argon atmosphere. After cooling down to room temperature, the polymer PBDTS-ID was precipitated in the presence of methanol (150 mL). The precipitate was then subjected to Soxhlet extraction with methanol, hexane, and toluene. The polymer was recovered as a black solid (187 mg, 70.7%) from the toluene fraction by precipitation from methanol. Anal. calcd. for C₈₂H₁₁₂N₂O₂S₆: C 72.99, H 8.30, O 2.37, N 2.07, S 14.25; found: C 72.80, H 8.44, O, 2.25, N 2.02, S 14.47.

2.4.2. Synthesis of PBDTS-DTNT

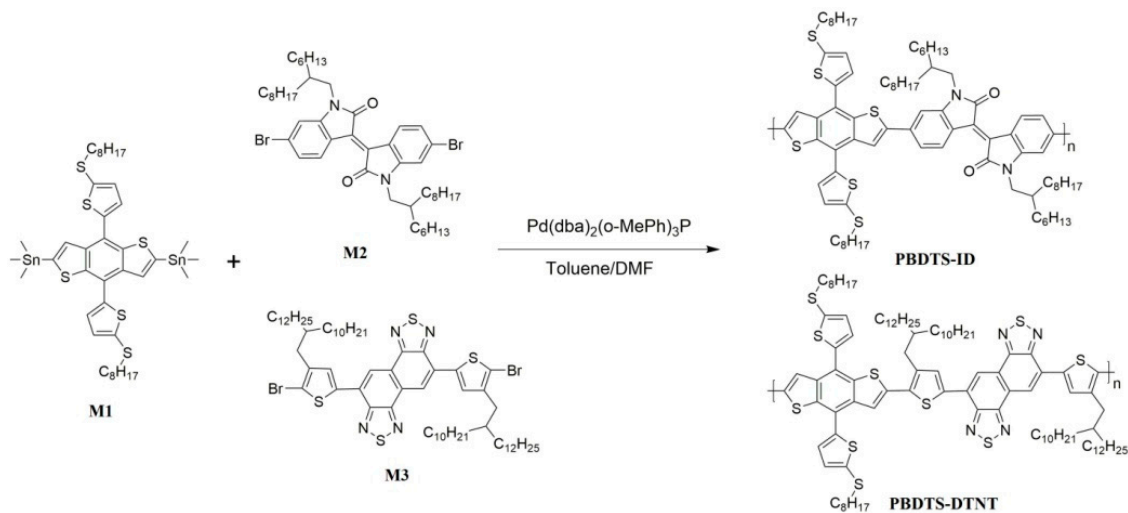
M1 (193.7 mg, 0.2 mmol), M3 (247.2 mg, 0.2 mmol), Pd(dba)₂ (3 mg), and tris(3-methoxyphenyl)phosphine (6 mg) were used to synthesize PBDTS-DTNT. The other experimental processes were the same as the preparation of the PBDTS-ID polymer described above. The target polymer, PBDTS-DTNT, was obtained as a dark solid (262 mg, 76.1%). Anal. calcd. for C₁₀₀H₁₄₂N₄S₁₀: C 69.79, H 8.32, N 3.26, S 18.63; found: C 70.32, H 8.24, N 2.95, S 19.03.

3. Results and Discussion

3.1. Synthesis and Characterization

M1, M2, and M3 were prepared according to the literature methods and their chemical structures were confirmed by NMR measurement (Figures S1–S3) [17,34,50]. The synthetic routes to the polymers PBDTS-ID and PBDTS-DTNT are outlined in Scheme 1. The polymers were prepared by Stille-coupling polymerization with distannyl and dibromide monomers using Pd(dba)₂ and tris(3-methoxyphenyl)phosphine as a catalyst. Both polymers are soluble in normal organic solvent such as toluene, chlorobenzene, and *o*-dichlorobenzene. Gel permeation chromatography (GPC) was applied to measure the average molecular weights using THF at room temperature. The *M_n* of PBDTS-ID and PBDTS-DTNT was 23.4 and 47.2 KDa, respectively, with a polydispersity index

of 1.78 and 2.10, respectively. Thermal properties of the two polymers were evaluated by TGA measurement (Figure 1), and the results suggested that both polymers exhibited good thermal stability, with decomposition temperatures (5% weight loss) of 348 and 335 °C for PBDTS-ID and PBDTS-DTNT, respectively.



Scheme 1. Synthetic routes for the polymers PBDTS-ID and PBDTS-DTNT.

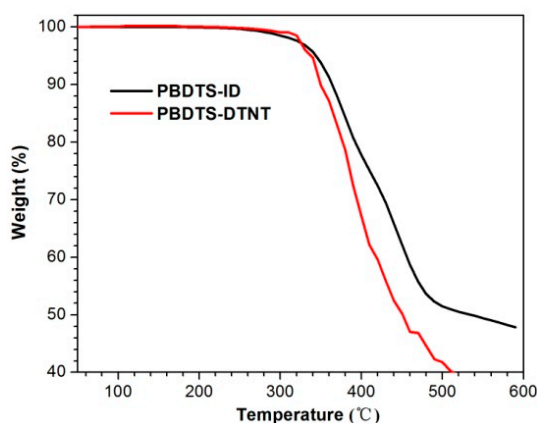


Figure 1. TGA curves of the polymers PBDTS-ID and PBDTS-DTNT.

3.2. Optical and Electrochemical Properties

Figure 2 exhibits the normalized UV-visible absorption spectra of the polymers PBDTS-ID and PBDTS-DTNT in dilute chloroform solution and thin films, respectively. The corresponding absorption parameters are summarized in Table 1. PBDTS-ID showed a broad absorption profile in the range from 300 to 783 nm, with a maximum absorption peak (λ_{\max}) at 720 nm (Figure 2a). Compared to PBDTS-ID, PBDTS-DTNT displayed an obviously broadened and red-shifted spectrum extended to the longer wavelength region (~816 nm), which can probably be ascribed to the enhanced electron-withdrawing ability for the acceptors DTNT [38]. In the solid state, the polymers exhibited almost identical absorption profiles but broadened absorption regions, with λ_{onset} of absorption edge values at 803 and 842 nm for PBDTS-ID and PBDTS-DTNT, respectively, which is 20 and 26 nm red-shifted compared to that of their solutions [54]. The optical bandgaps (E_g^{opt}) of the PBDTS-ID and PBDTS-DTNT estimated from absorption edges in the solid state were 1.54 and 1.47 eV according to $E_g^{\text{opt}} = 1240/\lambda_{\text{onset}}$, respectively.

Table 1. Optical and electrochemical properties of the polymers.

Polymers	λ_{onset} (nm)	$E_{\text{g}}^{\text{opt}}$ (eV) ¹	E_{HOMO} (eV) ²	E_{LUMO} (eV) ³
PBDTS-ID	803	1.54	−5.40	−3.86
PBDTS-DTNT	842	1.47	−5.24	−3.77

¹ Bandgap estimated from the absorption edge in thin film ($E_{\text{g}}^{\text{opt}} = 1240/\lambda_{\text{onset}}$ eV); ² The highest occupied molecular orbital (HOMO) level was estimated from cyclic voltammetry (CV) analysis; ³ The lowest unoccupied molecular orbital (LUMO) level was estimated by using the following equation: $E_{\text{LUMO}} = E_{\text{HOMO}} + E_{\text{g}}^{\text{opt}}$.

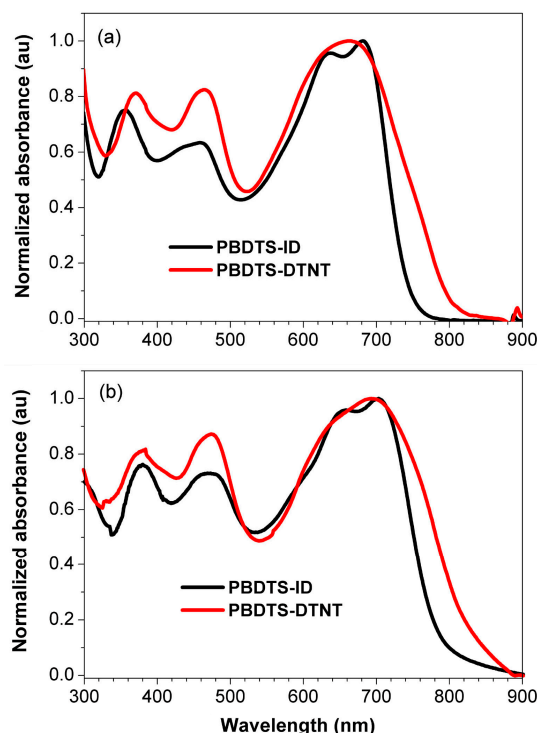


Figure 2. Normalized UV-visible absorption spectra of the polymers in chloroform solution (a) and thin solid films (b).

CV was employed to determine the energy level of the polymers in a three electrode electrochemical system. The acetonitrile solution containing $0.1 \text{ mol}\cdot\text{L}^{-1}$ tetrabutylammonium tetrafluoroborate (Bu_4NBF_4) was purged with argon for 5 min before CV measurement. The CV curve was obtained vs. the potential of an Ag/AgCl reference electrode, which was calibrated by the ferrocene-ferrocenium (Fc/Fc^+) redox couple (-4.8 eV to vacuum). The redox potential of Fc/Fc^+ in this study was found to be $+0.37 \text{ V}$ vs. the reference electrode. As shown in Figure 3, the onset oxidation potentials of PBDTS-ID and PBDTS-DTNT were observed at around 0.97 and 0.81 V , respectively. According to the empirical formula $E_{\text{HOMO}} = -e(E_{\text{ox}}^{\text{onset}} - E_{1/2}^{\text{ferrocene}} + 4.8)$ (eV), the corresponding HOMO energy levels of PBDTS-ID and PBDTS-DTNT were calculated to be -5.40 and -5.24 eV , respectively (Table 1). The HOMO level of PBDTS-ID is deeper than that of PBDTS-DTNT, which should be beneficial for obtaining a higher V_{OC} in PBDTS-ID-based PSCs. This will be discussed in detail below. The LUMO energy levels of the polymers PBDTS-ID and PBDTS-DTNT were -3.86 and -3.77 eV , respectively, calculated from the empirical formula $E_{\text{LUMO}} = E_{\text{HOMO}} + E_{\text{g}}^{\text{opt}}$.

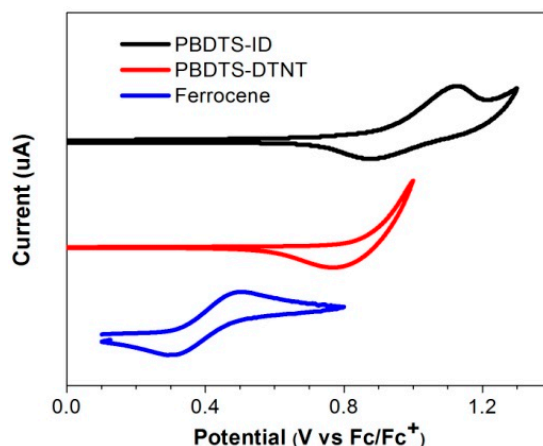


Figure 3. CV curves of the polymers PBDTS-ID and PBDTS-DTNT.

3.3. Hole Mobility

The hole-transport properties were a very important factor for polymer donor photovoltaic materials. To explore the hole mobility of the resulting polymers, we fabricated hole-only devices with a configuration of ITO/PEDOT:PSS/polymer:PC₇₁BM/MoO₃/Ag, and the hole mobilities were determined by using the space-charge-limited current (SCLC) method [14]. The hole mobility data were extracted by modeling the dark current and calculated from *J*–*V* characteristics fitted with the Mott–Gurney equation (Figure 4). The measured hole mobilities were determined to be 3.83×10^{-5} and $8.36 \times 10^{-5} \text{ cm}^2 \cdot \text{V}^{-1} \cdot \text{S}^{-1}$ for PBDTS-ID:PC₇₁BM and PBDTS-DTNT:PC₇₁BM blended films, respectively (Table 2).

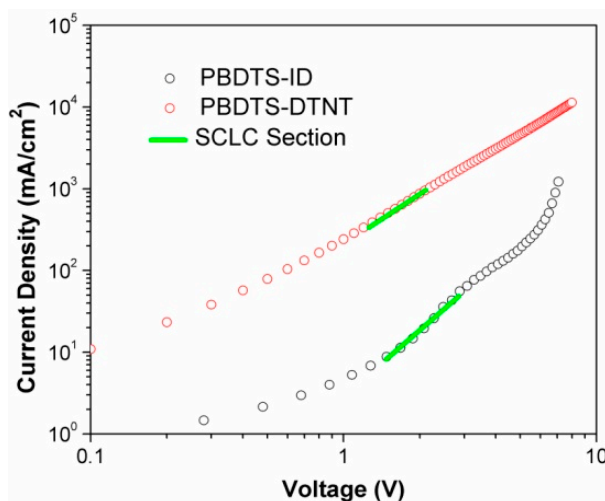


Figure 4. *J*–*V* curves of the hole-only devices under optimized conditions achieved by the space-charge-limited current (SCLC) method.

Table 2. Photovoltaic performance of the polymer solar cells (PSCs) fabricated by using the configuration of indium-tin oxide (ITO)/poly(ethylenimine ethoxylate) (PEIE)/polymer:PC₇₁BM/MoO₃/Ag.

Polymers	$\mu (\times 10^{-5}, \text{cm}^2 \cdot \text{V}^{-1} \cdot \text{S}^{-1})$	$J_{\text{SC}} (\text{mA} \cdot \text{cm}^{-2})$	$V_{\text{OC}} (\text{V})$	FF (%)	PCE (%)
PBDTS-ID	3.83	8.21	0.84	39.2	2.70
PBDTS-DTNT	8.36	8.31	0.72	45.8	2.71

3.4. Photovoltaic Performance

A solution-processed PSC was fabricated with the invert architecture of ITO/PEIE (10 nm)/active layer/MoO₃ (10 nm)/Ag (100 nm) to investigate the photovoltaic performance because the inverted device has demonstrated better ambient stability compare to the conventional device. The use of PEIE on the ITO substrate was found to improve the electron collection efficiency in the inverted device [55]. The active layer of the PSC was prepared from chlorobenzene blend solution of polymer and PC₇₁BM. The optimized ratios of PBDTS-ID:PC₇₁BM and PBDTS-DTNT:PC₇₁BM were 1:1.5 and 1:2, respectively, with 3% 1,8-diiodooctane (DIO) as the additive. The current *J*-*V* characteristics are shown in Figure 5a and the key device parameters are listed in Table 2. The PSC based on PBDTS-ID exhibited a moderate PCE of 2.70% with $V_{OC} = 0.84$ V, $J_{SC} = 8.21$ mA·cm⁻², and FF = 39.2%. Meanwhile, the PBDTS-DTNT-based PSC showed a similar PCE to the device of PBDTS-ID with a V_{OC} of 0.72 V, J_{SC} of 8.31 mA·cm⁻², and FF of 45.8%. From photovoltaic performance, the PBDTS-ID exhibited higher V_{OC} than that of the device based on PBDTS-DTNT. In addition to the factors such as shunt resistance and recombination dynamics, the difference between the HOMO of the polymer and the LUMO of the PC₇₁BM may also affect the V_{OC} . Thus, the deeper HOMO energy level can result in the higher V_{OC} in the PBDTS-ID-based device. However, the PSC based on PBDTS-ID displayed a lower FF of 39.2%, which could be ascribed to the lower hole mobility of PBDTS-ID. Meanwhile, the broadened absorption of PBDTS-DTNT shown in the external quantum efficiency (EQE) spectra (Figure 5b), which covered a larger fraction of the sunlight, might be considered as the important factor for the enhancement of the FF for PBDTS-DTNT.

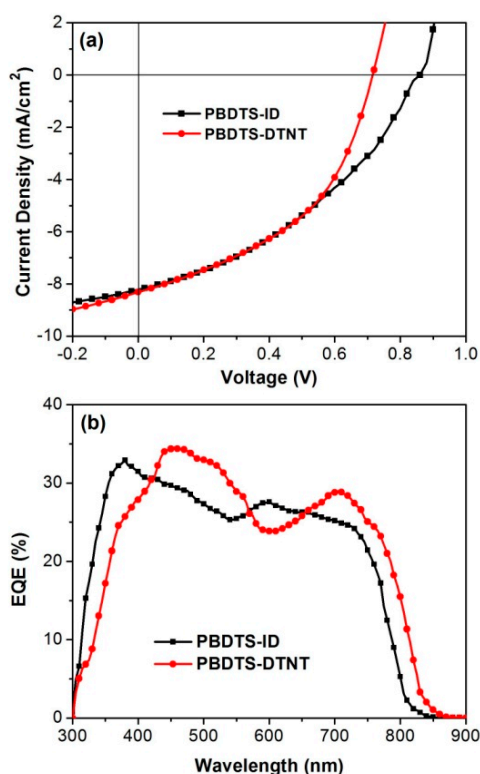


Figure 5. (a) *J*-*V* curves of the best-performing PSCs from the blend of the polymers and PC₇₁BM; (b) external quantum efficiency (EQE) curves of the corresponding PSCs with 3% 1,8-diiodooctane (DIO) additive treatment.

To verify the PCE of these devices, the EQE spectra of the devices under optimum conditions were investigated, as shown in Figure 5b. Both devices showed moderate photo-conversion efficiency in the wavelength range from 300 to 840 nm, with a maximum EQE value of 33% at 380 nm for PBDTS-ID

and a maximum EQE value of 35% at 467 nm for PBDTS-DTNT, respectively. The current densities integrated from EQE values of PBDTS-ID and PBDTS-DTNT were consistent with the result obtained from the J - V measurements.

3.5. Morphology Study

In order to better understand the factors affecting the device performance, we investigated the surface morphologies of blend films using AFM and TEM measurements, respectively. The experimental procedure for the preparation of the active layer is identical to those used to fabricate the polymer and PC₇₁BM blend film of the device. As shown in Figure 6, the active layers featured a grainy surface with high root mean square (RMS) roughness values of 8.26 and 7.52 nm for PBDTS-ID- and PBDTS-DTNT-based devices, respectively, suggesting serious phase separation. Under such conditions, photo-produced excitons cannot realize efficient dissociation and charge collection in the PSCs, causing an accompanied loss of photocurrent [14,18]. Therefore, the devices exhibited low J_{SC} and FF, and thus moderate PCEs.

The TEM measurement was applied to provide more information about the active layer. As shown in Figure 7a, larger fibrillar structures can be clearly found in the TEM image of the PBDTS-ID:PC₇₁BM blend film, which might diminish exciton dissociation and charge transport efficiency and is not favorable device performance [10,56]. However, relatively smaller size aggregations were observed in the TEM image (Figure 7b) of the PBDTS-DTNT:PC₇₁BM active layer compared to that of the PBDTS-ID:PC₇₁BM blend film (Figure 7a), which is consistent with the observations obtained from the AFM data.

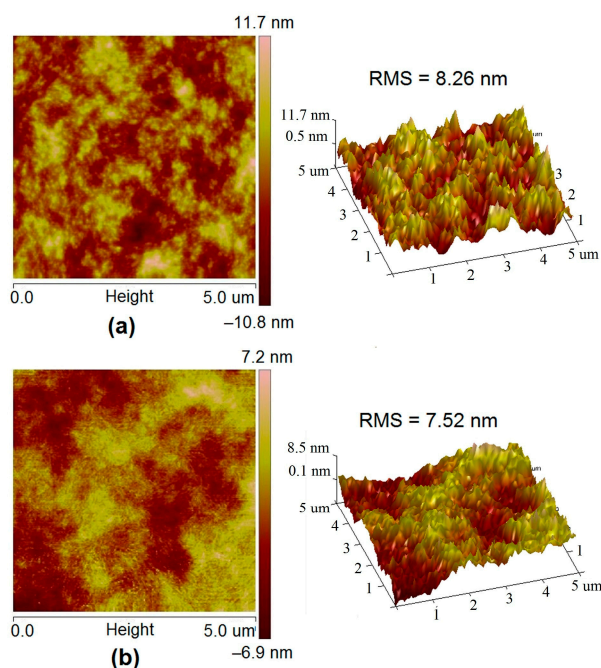


Figure 6. Atomic force microscopy (AFM) height images of PBDTS-ID:PC₇₁BM (a) and PBDTS-DTNT:PC₇₁BM (b) blend films with 3% DIO additive treatment.

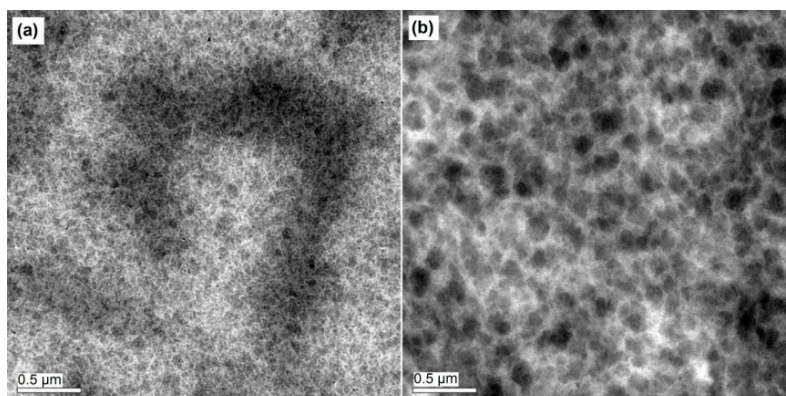


Figure 7. TEM images of PBDTS-ID:PC₇₁BM (a) and PBDTS-DTNT:PC₇₁BM (b) blend films with 3% DIO additive treatment.

4. Conclusions

In this paper, we synthesized two polymers containing alkylthiothienyl-substituted BDT donating units and ID or NT accepting units through Stille-coupling polymerization. PBDTS-ID and PBDTS-DTNT exhibited a broad absorption range in the solar spectrum, and the calculated optical band gaps were 1.54 and 1.47 eV, respectively. The polymers are both thermally stable and were used as donor materials in combination with PC₇₁BM in BHJ PSCs. The PSC devices prepared from PBDTS-ID and PBDTS-DTNT with the inverted structure of ITO/PEIE/polymer:PC₇₁BM/MoO₃/Ag showed maximum PCEs of 2.70% and 2.71%, respectively.

Overall, the photovoltaic performance of PBDTS-ID and PBDTS-DTNT was lower than that of many reported alkylthiothienyl-substituted BDT-based conjugated polymers, mainly because of the decreased current density. The positive results, such as suitable energy levels obtained for PBDTS-ID and PBDTS-DTNT, demonstrated that their photovoltaic performance might be increased by fine-tuning the structures of the conjugated polymers further.

Supplementary Materials: The following are available online at www.mdpi.com/2073-4360/10/3/331/s1, Figure S1: ¹H NMR spectrum of M1 in CDCl₃, Figure S2: ¹H NMR spectrum of M2 in CDCl₃, Figure S3: ¹H NMR spectrum of M3 in CDCl₃, Figure S4: X-ray diffraction patterns of blend films for the polymers.

Acknowledgments: This work was supported by Natural Science Foundation of China (Grant No. 51103111), Education Ministry of China (Program for NCET-12-0714), and the Scientific Research Foundation for Returned Overseas Chinese Scholars.

Author Contributions: Xunchang Wang conceived and performed the experiments; Xunchang Wang, Chang Cheng, and Yuda Li analyzed and discussed the data; Feng Wang and Xunchang Wang wrote the paper.

Conflicts of Interest: The authors declare no conflict of interest.

References

- Lu, L.Y.; Zheng, T.Y.; Wu, Q.H.; Schneider, A.M.; Zhao, D.L.; Yu, L.P. Recent advances in bulk heterojunction polymer solar cells. *Chem. Rev.* **2015**, *115*, 12666–12731. [[CrossRef](#)] [[PubMed](#)]
- Cheng, Y.J.; Yang, S.H.; Hsu, C.S. Synthesis of conjugated polymers for organic solar cell applications. *Chem. Rev.* **2009**, *109*, 5868–5923. [[CrossRef](#)] [[PubMed](#)]
- Yao, H.F.; Ye, L.; Zhang, H.; Li, S.S.; Zhang, S.Q.; Hou, J.H. Molecular design of benzodithiophene-based organic photovoltaic materials. *Chem. Rev.* **2016**, *116*, 7397–7457. [[CrossRef](#)] [[PubMed](#)]
- Wright, M.; Lin, R.; Tayebjee, M.J.Y.; Conibeer, G. Effect of blend composition on bulk heterojunction organic solar cells: A review. *Sol. RRL* **2017**, *1*, 31. [[CrossRef](#)]
- Cheng, P.; Zhan, X.W. Stability of organic solar cells: Challenges and strategies. *Chem. Soc. Rev.* **2016**, *45*, 2544–2582. [[CrossRef](#)] [[PubMed](#)]

6. Nielsen, C.B.; Holliday, S.; Chen, H.Y.; Cryer, S.J.; McCulloch, I. Non-fullerene electron acceptors for use in organic solar cells. *Acc. Chem. Res.* **2015**, *48*, 2803–2812. [[CrossRef](#)] [[PubMed](#)]
7. Wu, J.S.; Cheng, S.W.; Cheng, Y.J.; Hsu, C.S. Donor-acceptor conjugated polymers based on multifused ladder-type arenes for organic solar cells. *Chem. Soc. Rev.* **2015**, *44*, 1113–1154. [[CrossRef](#)] [[PubMed](#)]
8. Zhao, W.C.; Li, S.S.; Yao, H.F.; Zhang, S.Q.; Zhang, Y.; Yang, B.; Hou, J.H. Molecular optimization enables over 13% efficiency in organic solar cells. *J. Am. Chem. Soc.* **2017**, *139*, 7148–7151. [[CrossRef](#)] [[PubMed](#)]
9. Jiang, J.M.; Raghunath, P.; Lin, Y.C.; Lin, H.K.; Ko, C.L.; Su, Y.W.; Lin, M.C.; Wei, K.H. Linear solubilizing side chain substituents enhance the photovoltaic properties of two-dimensional conjugated benzodithiophene-based polymers. *Polymer* **2015**, *79*, 262–270. [[CrossRef](#)]
10. Kim, J.H.; Park, J.B.; Yoon, S.C.; Jung, I.H.; Hwang, D.H. Enhanced and controllable open-circuit voltage using 2D-conjugated benzodithiophene (BDT) homopolymers by alkylthio substitution. *J. Mater. Chem. C* **2016**, *4*, 2170–2177. [[CrossRef](#)]
11. Su, Q.; Tong, J.F.; Li, J.F.; Zhang, P.; Yang, C.Y.; Zhang, C.Z.; Wang, F.; Chen, D.J.; Xia, Y.J. Synthesis and characterization of alternating and random conjugated polymers derived from dithieno[2,3-*d*:2',3'-*d'*]benzo[1,2-*b*:4,5-*b'*]dithiophene and 2,1,3-benzothiadiazole derivatives. *Polym. J.* **2015**, *47*, 803–809. [[CrossRef](#)]
12. Tong, J.F.; Li, M.J.; An, L.L.; Li, J.F.; Xu, X.H.; Zhang, P.; Yang, C.Y.; Wang, F.; Xia, Y.J. Synthesis of π -extended dithienobenzodithiophene-containing medium bandgap copolymers and their photovoltaic application. *J. Macromol. Sci. Part A-Pure Appl. Chem.* **2015**, *52*, 934–941. [[CrossRef](#)]
13. Wang, X.C.; Su, Q.; Li, Y.D.; Cheng, C.; Xia, Y.J.; He, L.Y.; Li, H.; Shu, G.; Wang, F. Synthesis and photovoltaic properties of donor-acceptor conjugated polymers based on 4,7-dithienyl-2,1,3-benzothiadiazole functionalized silole. *Synth. Met.* **2016**, *220*, 433–439. [[CrossRef](#)]
14. Wang, X.C.; Tong, J.H.; Guo, P.Z.; Li, Y.D.; Li, H.; Xia, Y.J.; Wang, F. Low-bandgap conjugated polymers based on alkylthiothienyl-substituted benzodithiophene for efficient bulk heterojunction polymer solar cells. *Polymer* **2017**, *122*, 96–104. [[CrossRef](#)]
15. Yao, H.F.; Zhao, W.C.; Zheng, Z.; Cui, Y.; Zhang, J.Q.; Wei, Z.X.; Hou, J.H. PBDT-TSR: A highly efficient conjugated polymer for polymer solar cells with a regioregular structure. *J. Mater. Chem. A* **2016**, *4*, 1708–1713. [[CrossRef](#)]
16. Ye, L.; Zhang, S.Q.; Huo, L.J.; Zhang, M.J.; Hou, J.H. Molecular design toward highly efficient photovoltaic polymers based on two-dimensional conjugated benzodithiophene. *Acc. Chem. Res.* **2014**, *47*, 1595–1603. [[CrossRef](#)] [[PubMed](#)]
17. Ye, L.; Zhang, S.Q.; Zhao, W.C.; Yao, H.F.; Hou, J.H. Highly efficient 2D-conjugated benzodithiophene-based photovoltaic polymer with linear alkylthio side chain. *Chem. Mater.* **2014**, *26*, 3603–3605. [[CrossRef](#)]
18. Yu, T.; Xu, X.P.; Li, Y.; Li, Z.J.; Peng, Q. Side-chain influence of wide-bandgap copolymers based on naphtho[1,2-*b*:5,6-*b'*]bispyrazine and benzo[1,2-*b*:4,5-*b'*]dithiophene for efficient photovoltaic applications. *ACS Appl. Mater. Interfaces* **2017**, *9*, 18142–18150. [[CrossRef](#)] [[PubMed](#)]
19. Zhang, X.W.; Chen, L.X.; Wang, G.; Zhang, Z.G.; Li, Y.F.; Shen, P. Synthesis and photovoltaic properties of alkylthiothienyl-substituted benzo[1,2-*b*:4,5-*b'*]dithiophene D-A copolymers with different accepting units. *Synth. Met.* **2016**, *211*, 121–131. [[CrossRef](#)]
20. Zhu, E.W.; Ge, G.D.; Shu, J.K.; Yi, M.D.; Bian, L.Y.; Hai, J.F.; Yu, J.S.; Liu, Y.; Zhou, J.; Tang, W.H. Direct access to 4,8-functionalized benzo[1,2-*b*:4,5-*b'*]dithiophenes with deep low-lying HOMO levels and high mobilities. *J. Mater. Chem. A* **2014**, *2*, 13580–13586. [[CrossRef](#)]
21. Cao, K.C.; Wu, Z.W.; Li, S.G.; Sun, B.Q.; Zhang, G.B.; Zhang, Q. A low bandgap polymer based on isoindigo and bis(dialkylthienyl)benzodithiophene for organic photovoltaic applications. *J. Polym. Sci. Pol. Chem.* **2013**, *51*, 94–100. [[CrossRef](#)]
22. Zhang, M.J.; Guo, X.; Zhang, S.Q.; Hou, J.H. Synergistic effect of fluorination on molecular energy level modulation in highly efficient photovoltaic polymers. *Adv. Mater.* **2014**, *26*, 1118–1123. [[CrossRef](#)] [[PubMed](#)]
23. Chen, W.C.; Xiao, M.J.; Han, L.L.; Zhang, J.D.; Jiang, H.X.; Gu, C.T.; Shen, W.F.; Yang, R.Q. Unsubstituted benzodithiophene-based conjugated polymers for high-performance organic field-effect transistors and organic solar cells. *ACS Appl. Mater. Interfaces* **2016**, *8*, 19665–19671. [[CrossRef](#)] [[PubMed](#)]
24. Liu, D.Y.; Zhu, Q.Q.; Gu, C.Y.; Wang, J.Y.; Qiu, M.; Chen, W.C.; Bao, X.C.; Sun, M.L.; Yang, R.Q. High-performance photovoltaic polymers employing symmetry-breaking building blocks. *Adv. Mater.* **2016**, *28*, 8490–8498. [[CrossRef](#)] [[PubMed](#)]

25. Kan, B.; Zhang, Q.; Li, M.M.; Wan, X.J.; Ni, W.; Long, G.K.; Wang, Y.C.; Yang, X.; Feng, H.R.; Chen, Y.S. Solution-processed organic solar cells based on dialkylthiol-substituted benzodithiophene unit with efficiency near 10%. *J. Am. Chem. Soc.* **2014**, *136*, 15529–15532. [[CrossRef](#)] [[PubMed](#)]
26. Xu, X.F.; Li, Z.J.; Zhang, W.; Meng, X.Y.; Zou, X.S.; Rasi, D.D.; Ma, W.; Yartsev, A.; Andersson, M.R.; Janssen, R.A.J.; et al. 8.0% efficient all-polymer solar cells with high photovoltage of 1.1 v and internal quantum efficiency near unity. *Adv. Energy Mater.* **2018**, *8*, 11. [[CrossRef](#)]
27. Lu, L.Y.; Yu, L.P. Understanding low bandgap polymer PTB7 and optimizing polymer solar cells based on it. *Adv. Mater.* **2014**, *26*, 4413–4430. [[CrossRef](#)] [[PubMed](#)]
28. Lee, D.; Stone, S.W.; Ferraris, J.P. A novel dialkylthiobenzo[1,2-*b*:4,5-*b'*]dithiophene derivative for high open-circuit voltage in polymer solar cells. *Chem. Commun.* **2011**, *47*, 10987–10989. [[CrossRef](#)] [[PubMed](#)]
29. Huang, Y.; Guo, X.; Liu, F.; Huo, L.J.; Chen, Y.N.; Russell, T.P.; Han, C.C.; Li, Y.F.; Hou, J.H. Improving the ordering and photovoltaic properties by extending π -conjugated area of electron-donating units in polymers with D-A structure. *Adv. Mater.* **2012**, *24*, 3383–3389. [[CrossRef](#)] [[PubMed](#)]
30. Cui, C.H.; Wong, W.Y.; Li, Y.F. Improvement of open-circuit voltage and photovoltaic properties of 2D-conjugated polymers by alkylthio substitution. *Energy Environ. Sci.* **2014**, *7*, 2276–2284. [[CrossRef](#)]
31. Liu, T.; Pan, X.X.; Meng, X.Y.; Liu, Y.; Wei, D.H.; Ma, W.; Huo, L.J.; Sun, X.B.; Lee, T.H.; Huang, M.; et al. Alkyl side-chain engineering in wide-bandgap copolymers leading to power conversion efficiencies over 10%. *Adv. Mater.* **2017**, *29*, 7. [[CrossRef](#)] [[PubMed](#)]
32. Ho, C.C.; Chen, C.A.; Chang, C.Y.; Darling, S.B.; Su, W.F. Isoindigo-based copolymers for polymer solar cells with efficiency over 7%. *J. Mater. Chem. A* **2014**, *2*, 8026–8032. [[CrossRef](#)]
33. Jung, I.H.; Kim, J.H.; Nam, S.Y.; Lee, C.; Hwang, D.H.; Yoon, S.C. A di(1-benzothieno)[3,2-*b*:2',3'-*d*]pyrrole and isoindigo-based electron donating conjugated polymer for efficient organic photovoltaics. *J. Mater. Chem. C* **2016**, *4*, 663–667. [[CrossRef](#)]
34. Lei, T.; Wang, J.Y.; Pei, J. Design, synthesis, and structure-property relationships of isoindigo-based conjugated polymers. *Acc. Chem. Res.* **2014**, *47*, 1117–1126. [[CrossRef](#)] [[PubMed](#)]
35. Liu, C.C.; Dong, S.; Cai, P.; Liu, P.; Liu, S.J.; Chen, J.W.; Liu, F.; Ying, L.; Russell, T.P.; Huang, F.; et al. Donor-acceptor copolymers based on thermally cleavable indigo, isoindigo, and DPP units: Synthesis, field effect transistors, and polymer solar cells. *ACS Appl. Mater. Interfaces* **2015**, *7*, 9038–9051. [[CrossRef](#)] [[PubMed](#)]
36. Ma, Z.F.; Dang, D.F.; Tang, Z.; Gedefaw, D.; Bergqvist, J.; Zhu, W.G.; Mammo, W.; Andersson, M.R.; Inganäs, O.; Zhang, F.L.; et al. A facile method to enhance photovoltaic performance of benzodithiophene-isoindigo polymers by inserting bithiophene spacer. *Adv. Energy Mater.* **2014**, *4*. [[CrossRef](#)]
37. Stalder, R.; Grand, C.; Subbiah, J.; So, F.; Reynolds, J.R. An isoindigo and dithieno[3,2-*b*:2',3'-*d*]silole copolymer for polymer solar cells. *Polym. Chem.* **2012**, *3*, 89–92. [[CrossRef](#)]
38. Tong, J.F.; An, L.L.; Li, J.F.; Zhang, P.; Guo, P.Z.; Yang, C.Y.; Su, Q.; Wang, X.C.; Xia, Y.J. Large branched alkylthienyl bridged naphtho[1,2-*c*:5,6-*c'*]bis[1,2,5]thiadiazole-containing low bandgap copolymers: Synthesis and photovoltaic application. *J. Macromol. Sci. Part A Pure Appl. Chem.* **2017**, *54*, 176–185. [[CrossRef](#)]
39. Tong, J.F.; Li, J.F.; Zhang, P.; Ma, X.Y.; Wang, M.; An, L.L.; Sun, J.B.; Guo, P.Z.; Yang, C.Y.; Xia, Y.J. Naphtho[1,2-*c*:5,6-*c'*]bis[1,2,5]thiadiazole-based conjugated polymers consisting of oligothiophenes for efficient polymer solar cells. *Polymer* **2017**, *121*, 183–195. [[CrossRef](#)]
40. Wang, E.G.; Mammo, W.; Andersson, M.R. 25th anniversary article: Isoindigo-based polymers and small molecules for bulk heterojunction solar cells and field effect transistors. *Adv. Mater.* **2014**, *26*, 1801–1826. [[CrossRef](#)] [[PubMed](#)]
41. Wang, Z.G.; Zhao, J.; Li, Y.; Peng, Q. Low band-gap copolymers derived from fluorinated isoindigo and dithienosilole: Synthesis, properties and photovoltaic applications. *Polym. Chem.* **2014**, *5*, 4984–4992. [[CrossRef](#)]
42. Zheng, Y.Q.; Wang, Z.; Dou, J.H.; Zhang, S.D.; Luo, X.Y.; Yao, Z.F.; Wang, J.Y.; Pei, J. Effect of halogenation in isoindigo-based polymers on the phase separation and molecular orientation of bulk heterojunction solar cells. *Macromolecules* **2015**, *48*, 5570–5577. [[CrossRef](#)]
43. Chatterjee, S.; Ie, Y.; Karakawa, M.; Aso, Y. Naphtho[1,2-*c*:5,6-*c'*]bis[1,2,5]thiadiazole-containing π -conjugated compound: Nonfullerene electron acceptor for organic photovoltaics. *Adv. Funct. Mater.* **2016**, *26*, 1161–1168. [[CrossRef](#)]

44. Jin, Y.C.; Chen, Z.M.; Xiao, M.J.; Peng, J.J.; Fan, B.B.; Ying, L.; Zhang, G.C.; Jiang, X.F.; Yin, Q.W.; Liang, Z.Q.; et al. Thick film polymer solar cells based on naphtho[1,2-*c*:5,6-*c'*]bis[1,2,5]thiadiazole conjugated polymers with efficiency over 11%. *Adv. Energy Mater.* **2017**, *7*. [[CrossRef](#)]
45. Li, W.; Li, Q.D.; Liu, S.J.; Duan, C.H.; Ying, L.; Huang, F.; Cao, Y. Synthesis of two-dimensional π -conjugated polymers pendent with benzothiadiazole and naphtho[1,2-*c*:5,6-*c'*]bis[1,2,5]thiadiazole moieties for polymer solar cells. *Sci. China Chem.* **2015**, *58*, 257–266. [[CrossRef](#)]
46. Liu, L.Q.; Zhang, G.C.; He, B.T.; Huang, F. Polymer solar cells based on the copolymers of naphtho[1,2-*c*:5,6-*c'*]bis(1,2,5-thiadiazole) and alkoxyphenyl substituted benzodithiophene with high open-circuit voltages. *Chin. J. Chem.* **2015**, *33*, 902–908. [[CrossRef](#)]
47. Liu, L.Q.; Zhang, G.C.; Liu, P.; Zhang, J.; Dong, S.; Wang, M.; Ma, Y.G.; Yip, H.L.; Huang, F. Donor-acceptor-type copolymers based on a naphtho[1,2-*c*:5,6-*c'*]bis(1,2,5-thiadiazole) scaffold for high-efficiency polymer solar cells. *Chem. -Asian J.* **2014**, *9*, 2104–2112. [[CrossRef](#)] [[PubMed](#)]
48. Osaka, I.; Shimawaki, M.; Mori, H.; Doi, I.; Miyazaki, E.; Koganezawa, T.; Takimiya, K. Synthesis, characterization, and transistor and solar cell applications of a naphthobisthiadiazole-based semiconducting polymer. *J. Am. Chem. Soc.* **2012**, *134*, 3498–3507. [[CrossRef](#)] [[PubMed](#)]
49. Sun, Y.M.; Seifert, J.; Wang, M.; Perez, L.A.; Luo, C.; Bazan, G.C.; Huang, F.; Cao, Y.; Heeger, A.J. Effect of molecular order on the performance of naphthobisthiadiazole-based polymer solar cells. *Adv. Energy Mater.* **2014**, *4*. [[CrossRef](#)]
50. Wang, M.; Hu, X.W.; Liu, P.; Li, W.; Gong, X.; Huang, F.; Cao, Y. Donor acceptor conjugated polymer based on naphtho[1,2-*c*:5,6-*c'*]bis[1,2,5]thiadiazole for high-performance polymer solar cells. *J. Am. Chem. Soc.* **2011**, *133*, 9638–9641. [[CrossRef](#)] [[PubMed](#)]
51. Yasuda, T.; Shinohara, Y.; Kusagaki, Y.; Matsuda, T.; Han, L.; Ishi-I, T. Synthesis and photovoltaic properties of naphthobisthiadiazole-triphenylamine-based donor-acceptor π -conjugated polymer. *Polymer* **2015**, *58*, 139–145. [[CrossRef](#)]
52. Zhang, L.H.; Pei, K.; Yu, M.D.; Huang, Y.L.; Zhao, H.B.; Zeng, M.; Wang, Y.; Gao, J.W. Theoretical investigations on donor-acceptor conjugated copolymers based on naphtho[1,2-*c*:5,6-*c'*]bis[1,2,5]thiadiazole for organic solar cell applications. *J. Phys. Chem. C* **2012**, *116*, 26154–26161. [[CrossRef](#)]
53. Zhu, X.W.; Fang, J.; Lu, K.; Zhang, J.Q.; Zhu, L.Y.; Zhao, Y.F.; Shuai, Z.G.; Wei, Z.X. Naphtho[1,2-*b*:5,6-*b'*]dithiophene based two-dimensional conjugated polymers for highly efficient thick-film inverted polymer solar cells. *Chem. Mater.* **2014**, *26*, 6947–6954. [[CrossRef](#)]
54. Li, Y.D.; Zhang, H.; Wang, X.C.; Wang, F.; Xia, Y.J. Synthesis and photovoltaic properties of silole-containing conjugated polymers. *Acta Chim. Sin.* **2015**, *73*, 1055–1060.
55. Liu, T.F.; Jiang, F.Y.; Tong, J.H.; Qin, F.; Meng, W.; Jiang, Y.Y.; Li, Z.F.; Zhou, Y.H. Reduction and oxidation of poly(3,4-ethylenedioxythiophene):Poly(styrenesulfonate) induced by methylamine (CH₃NH₂)-containing atmosphere for perovskite solar cells. *J. Mater. Chem. A* **2016**, *4*, 4305–4311. [[CrossRef](#)]
56. Zhang, S.Q.; Uddin, M.A.; Zhao, W.C.; Ye, L.; Woo, H.Y.; Liu, D.L.; Yang, B.; Yao, H.F.; Cui, Y.; Hou, J.H. Optimization of side chains in alkylthiophene-substituted benzo[1,2-*b*:4,5-*b'*]dithiophene-based photovoltaic polymers. *Polym. Chem.* **2015**, *6*, 2752–2760. [[CrossRef](#)]

